Environmental Technology & Innovation 28 (2022) 102636

Contents lists available at ScienceDirect

Environmental Technology & Innovation

journal homepage: www.elsevier.com/locate/eti

Removal of heavy metals from stormwater runoff using granulated drinking water treatment residuals

Viravid Na Nagara [a], Dibyendu Sarkar [a,*], Evert J. Elzinga [b], Rupali Datta [c]

[a] Department of Civil, Environmental and Ocean Engineering, Stevens Institute of Technology, Hoboken, NJ, USA
[b] Department of Earth & Environmental Sciences, Rutgers University, Newark, NJ, USA
[c] Department of Biological Sciences, Michigan Technological University, Houghton, MI, USA

ARTICLE INFO

Article history:
Received 23 February 2022
Received in revised form 23 April 2022
Accepted 27 April 2022
Available online 6 May 2022

Keywords:
Waste-to-resource
Water treatment
Sorbent
Stormwater pollution
Surface complexation model

ABSTRACT

Stormwater runoff is a significant source of heavy metals, including cadmium (Cd), chromium (Cr), and nickel (Ni), which pose ecological and human health problems. Various filter media have been evaluated for heavy metal removal from stormwater via adsorption, most involving chemical- or energy-intensive processes. Aluminum-based drinking water treatment residuals (WTR), a non-hazardous byproduct of drinking water treatment, are an inexpensive sorbent for heavy metals. However, the low permeability of WTR is a problem and requires mixing with sand and carbon materials to improve flow; but such amendments also reduce its sorption capacity. To overcome this problem, a granulated WTR sorbent was generated using a green technique involving organic materials and a low-energy process. Batch studies showed that WTR granules remove Cd, Cr, and Ni simultaneously. Metal removal was adequately described by pseudo-second-order kinetic models and Langmuir and Freundlich isotherm models. The overall removal performance was Cr > Cd > Ni. The presence of divalent cations in solution negatively affected metal removal; anions had a strong effect on Cd removal. A triple-layer surface complexation model adequately described metal removal. Results demonstrated the strong potential of the WTR granules to emerge as green filter media for the removal of heavy metals from stormwater runoff.

1. Introduction

Water pollution by heavy metals has been a major environmental concern due to their nonbiodegradability and high toxicity. Among various heavy metals, cadmium (Cd), chromium (Cr), and nickel (Ni), can be hazardous even at low concentrations (Rahman and Singh, 2019). Exposure to cadmium causes lung cancer and osteomalacia. Chromium, particularly Cr(VI), is toxic and can affect the central nervous system and cause kidney and liver damage. Excessive exposure to nickel may lead to cancer, nervous system damage, and a reduction in cell growth (Sharma, 2015).

Stormwater runoff is recognized as a significant source of heavy metals, which mainly come from traffic-related sources, such as tire wear, brake linings, engine, and vehicle bodywear (Huber et al., 2016; McKenzie et al., 2009; Müller

Abbreviations: BMP, best management practice; DI, deionized; FTIR, Fourier transform infrared spectroscopy; ICP-OES, inductively coupled plasma-optical emission spectrometer; PFO, pseudo-first-order; PSO, pseudo-second-order; SCM, surface complexation model; SEM-EDS, scanning electron microscope-energy dispersion spectroscopy; SSA, specific surface area; TCLP, toxicity characteristic leaching procedure; TLM, triple-layer model; WTR, aluminum-based drinking water treatment residuals

* Corresponding author.
E-mail address: dsarkar@stevens.edu (D. Sarkar).

https://doi.org/10.1016/j.eti.2022.102636

et al., 2020). In urban environments, heavy metals together with other anthropogenic pollutants on impervious surfaces are washed off by stormwater runoff and typically discharged to existing water bodies (e.g., rivers and lakes) or, without treatment, into groundwater (Göbel et al., 2007).

Stormwater best management practices (BMPs), including green infrastructures, have increasingly gained attention from practitioners in recent years, who have focused on the mitigation of various stormwater-related problems, primarily hydrologic issues such as flooding. However, these mitigation measures have limited capability to remove heavy metals, especially dissolved heavy metals, which are more bioavailable and more difficult to remove compared to particulate-bound heavy metals (Alam et al., 2018; Cederkvist et al., 2013; Flanagan et al., 2019; Lange et al., 2020; Maniquiz-Redillas and Kim, 2016). Therefore, economical and effective technologies are imperative for the treatment of dissolved heavy metals in stormwater.

Sorption is considered an economical and effective process for removing dissolved pollutants with the advantages of minimal waste generation, low footprint, and low energy requirement (Kumar et al., 2019; Søberg et al., 2019). Therefore, previous studies evaluated various materials (e.g., sand, compost, biochar, chalk, pumice stone, agricultural and industrial waste byproducts) for their effectiveness as sorbents in metal removal from stormwater facilities (Esfandiar et al., 2022; Søberg et al., 2019). However, most of these studies generally evaluated sorbents for their removal efficiency as a powder or loose material (Chakraborty et al., 2020; Rafatullah et al., 2010; Shimabuku et al., 2016), which are not suitable for implementation in stormwater treatment in most cases. The challenge in encapsulating or affixing the sorbent, which is the critical process toward successful implementation, remains and will ultimately affect the overall removal efficiency of the sorbents.

In this study, aluminum-based water treatment residuals (WTR) were utilized for generating sorbent granules. WTR is a byproduct of drinking water treatment facilities that use aluminum salts as coagulants. Every year, large quantities of WTR are generated across the world. In Japan, 290,000 tons of WTR were generated in 2011. The annual WTR generation in Netherland in 2014 and the UK in 2013 were 328,000 and 131,000 tons, respectively. In addition, the annual WTR generation in Scotland is expected to increase to 390,000 tons by 2025, which is a substantial increase compared to 310,000 tons in 2005 (Zhao et al., 2018).

Due to the increasing generation of WTR, reuse is imperative due to economic and environmental constraints on landfilling, which is its common method of disposal. WTR generally contains Al (oxy)hydroxides, activated carbon, and natural organic matter, which are suitable substances to promote sorption processes for reducing trace metal mobility in soil and waters (Castaldi et al., 2015). The effectiveness of WTR in removing environmental pollutants was investigated in many previous studies (Duan and Fedler, 2021; Makris et al., 2005, 2006; Na Nagara et al., 2021; Nagar et al., 2010). Based on Toxicity Characteristic Leaching Procedure (TCLP) results, the concentration of the toxic heavy metals in the leachate from WTR is well below regulatory limits, confirming that WTR is a non-hazardous material (Sarkar et al., 2020). Considerable advancements in application of WTR has been made in the past decade (Turner et al., 2019; Xu et al., 2020). WTR was investigated for use in various applications as remediation agents, such as wetland medium (Hu et al., 2012), coating material on wood mulch (Sidhu et al., 2020; Soleimanifar et al., 2016, 2019), catch basin filter amendment (Na Nagara et al., 2021), and bioretention amendment (Liu and Davis, 2014). Therefore, WTR is suitable for developing sorbent material from economic, environmental, and technical standpoints.

Although pollutant removal performance is the key focus of sorbent development, the hydraulic characteristics of the materials must be taken into account to prevent adverse influence on the flow of stormwater when implemented. Since WTR is a clay-like material with very low permeability, modification or amendment is required to improve its hydraulic conductivity. In our previous study, WTR was amended with sand and carbon material (Na Nagara et al., 2021). However, amending and mixing approaches pose a trade-off between flow and sorption performance since the amendments are less efficient in removing heavy metals compared to WTR. Therefore, encapsulation of WTR was selected as a suitable approach to improve hydraulic conductivity when implementing it as a sorbent material. In this study, WTR was encapsulated with calcium alginate using organic materials and a low energy process as described in the U.S. Patent Application Publication No. US 2020/0316556 A1 (Sarkar et al., 2020). Therefore, the resulting product, the WTR granules, is considered "green" from both economic and environmental perspectives.

The objectives of this study were to (i) investigate the physicochemical characteristics of the WTR granules; (ii) evaluate the Cd, Cr, and Ni removal performance of the WTR granules through kinetics, and sorption isotherms; (iii) investigate the effects of background ions, ionic strength, and pH on Cd, Cr, and Ni removal by sorption edge experiments; and (iv) understand the mechanisms that regulate the sorption of the three heavy metals and develop surface complexation models to predict the removal performance before implementation in stormwater facilities.

2. Materials and methods

2.1. Materials

Stock solutions of Cd, Cr, and Ni were prepared by dissolving their respective salts: $Cd(NO_3)_2 \bullet 4H_2O$ (Sigma-Aldrich, MO, USA), $K_2Cr_2O_7$ (Sigma-Aldrich, MO, USA), and $Ni(NO_3)_2 \bullet 6H_2O$ (Spectrum Chemical Mfg., NJ, USA) in deionized (DI) water. NaOH, HNO_3, NaCl, $NaNO_3$, KCl, $CaCl_2$, and $MgCl_2$ were acquired from Fisher Scientific (NJ, USA). Certified reference solutions were purchased from High-Purity Standards (SC, USA). Deionized (DI) water (electrical resistivity >18.2 MΩ) was used for preparing all solutions throughout the study. WTR was collected from the New Jersey American Water (NJAW) Water Treatment Plant in Bridgewater Township, NJ, USA, where aluminum salts are used as the main coagulant.

2.2. WTR granules generation

WTR granules were generated by following the method described in the U.S. Patent Application Publication No. US 2020/0316556 A1 (Sarkar et al., 2020). In brief, WTR was air-dried, followed by grinding and passing through a 1 mm sieve. The <1 mm fraction was milled by a planetary ball mill (Fritsch Pulverisette 5, Fritsch GmbH, Idar-Oberstein, Germany) at 290 rpm (tray rotating) and 590 rpm (grinding jar rotating) for 18 min. The milled WTR was added to a potassium alginate (BOC Sciences, NY, USA) solution. The WTR-alginate solution was added dropwise to a calcium solution prepared using eggshell powder to generate the WTR granules. The granules were washed several times with DI water until no residue from the calcium solution was present.

2.3. WTR granules characterization

The surface morphology and elemental semi-quantitative analysis of the samples were done by scanning electron microscope-energy dispersion spectroscopy (SEM-EDS; Auriga Small Dual-Beam FIB-SEM, Carl Zeiss, Jena, Germany; coupled with an 80 mm^2 silicon drift detector EDS system, Oxford Instruments, MA, USA). The surface chemical properties of the samples were characterized by Fourier transform infrared spectroscopy (FTIR Spectrometer, PerkinElmer Spectrum 100, MA, USA), with spectra recorded between 400 and 4000 cm^{-1}. Sample pellets were prepared for transmission analyses with fused-KBr with an equal amount of KBr for all samples at a 10:1 ratio. A total of 25 scans were averaged for each sample and the resolution was 4 cm^{-1}. The spectra were analyzed using OMNIC 9 software (Thermo Fisher Scientific Inc., MA, USA). The specific surface area (SSA) was evaluated using a surface area analyzer (Micromeritics ASAP 2020, GA, USA) where nitrogen was used as absorbent.

2.4. Kinetic study

The kinetic study was conducted in 1-L bottles containing 800 mL of synthetic stormwater to provide adequate headspace for mixing. The synthetic stormwater was prepared by diluting the prepared stock solutions in deionized water to achieve the target concentrations of 35, 85, and 100 μg/L for Cd, Cr, and Ni, respectively. The concentration of Cd, Cr, and Ni was determined based on their typical concentrations in stormwater runoff as reported in Huber et al. (2016). Sodium nitrate ($NaNO_3$) was used as a background electrolyte at the concentration of 0.1 M. The pH of the solutions was adjusted to pH 7.0 using HNO_3 and NaOH. pH buffer was not used to maintain the experiment at a constant pH since it would not be realistic and would suppress the surface complexation of the metals (Smičiklas et al., 2009). WTR granules (8 g) were loaded into the bottles. During the experiment, the bottles were placed on a rotary shaker at 180 rpm. Representative samples were collected at different times (5, 10, 20, 30 min, and 1, 2, 4, 6, 8, 12, 24, 36 h), filtered through a 0.45-μm nylon syringe filter, and analyzed using an inductively coupled plasma-optical emission spectrometer (ICP-OES, 5100 Agilent Technologies, CA, USA).

2.5. Sorption isotherm study

To evaluate the effectiveness of the WTR granules and determine equilibrium sorption parameters, a sorption isotherm experiment was performed. The WTR granules (1% w/v) were placed in 50-mL centrifuge tubes with 40 mL of the synthetic stormwater with a single pollutant at varying concentrations. The pH of the solutions was adjusted to pH 7.0 using HNO_3 and NaOH. The centrifuge tubes were placed on a rotary shaker at 180 rpm for 48 h at room temperature (23 °C ± 1 °C). After the designated time, samples were collected, filtered through a 0.45-μm nylon syringe filter, and analyzed using the ICP-OES.

2.6. Effect of environmental parameters

The effect of environmental parameters, including background electrolytes ($NaNO_3$, NaCl, KCl, $CaCl_2$, $MgCl_2$) and ionic strength (0 to 0.1 M), were investigated at a fixed pH (pH 7) and fixed initial concentrations of the metals (5 mg/L). The effect of the environmental parameters was performed by following the same procedure as used in the sorption isotherm study. Each environmental parameter was evaluated in a separate set of samples. When they were not subjected to variation, the background electrolyte was $NaNO_3$ with an ionic strength of 0.1 M. After 48 h, samples were collected, filtered through a 0.45-μm nylon syringe filter, and analyzed using the ICP-OES.

2.7. Sorption edge study

Solution pH is one of the most influencing factors on sorption characteristics. To understand the effect of pH on Cd, Cr, and Ni sorption, sorption edge study was performed by following the same procedure as used in the sorption isotherm study, except the target concentrations of the heavy metals were kept constant at 5 mg/L while the solution pH was varied in the range of 5.2 to 7.9 using HNO_3 and NaOH. This pH range was determined based on the typical pH range documented in the literature (Göbel et al., 2007).

2.8. Modeling

Based on the experimental data obtained, models were developed for the kinetic, sorption isotherm, and sorption edge studies. The kinetic data were used to perform kinetic modeling, which leads to suitable rate expressions characteristic of possible reaction mechanisms and allows estimation of sorption rates. In this study, the pseudo-first-order (PFO) equation (Lagergren, 1898), pseudo-second-order (PSO) equation (Blanchard et al., 1984), and intraparticle diffusion model (Weber and Morris, 1963) were considered. The mathematical expression of the models and related parameters are presented as follows:
The amount of each metal adsorbed by the WTR granules at equilibrium (q_e):

$$q_e = \frac{(C_0 - C_e)\,V}{m} \tag{1}$$

The amount of each metal adsorbed by the WTR granules at time t (q_t):

$$q_t = \frac{(C_0 - C_t)\,V}{m} \tag{2}$$

The pseudo-first-order (PFO) equation:

$$\ln(q_e - q_t) = -k_1 t + ln(q_e) \tag{3}$$

The pseudo-second-order (PSO) equation:

$$\frac{t}{q_t} = \frac{1}{q_e}t + \frac{1}{k_2 q_e^2} \tag{4}$$

The intraparticle diffusion equation:

$$q_t = k_i t^{0.5} + C \tag{5}$$

where C_0, C_e, C_t are the initial concentrations, equilibrium concentrations, and concentrations at time t of adsorbate in bulk solution, respectively; V is the volume of bulk solution; m is the mass of adsorbent. t is contact time, k_1 and k_2 are the PFO and PSO rate constants, k_i is the intraparticle diffusion rate constant, and C is the intercept.

The sorption isotherm data were fitted against the two most commonly used isotherm models: Langmuir (1918) and Freundlich (1907). The Langmuir equation is considered the most common and simplest model assuming monolayer adsorption, while the Freundlich model is an empirical model used to represent heterogeneous systems. The models are represented mathematically as follows:
The Langmuir isotherm model:

$$q_e = \frac{Q^0_{max} K_L C_e}{1 + K_L C_e} \tag{6}$$

The linearized Langmuir isotherm model:

$$\frac{1}{q_e} = \left(\frac{1}{Q^0_{max} K_L}\right)\frac{1}{C_e} + \frac{1}{Q^o_{max}} \tag{7}$$

The Freundlich isotherm model:

$$q_e = K_F C_e^{1/n} \tag{8}$$

The linearized Freundlich isotherm model:

$$\ln(q_e) = \ln(K_F) + \frac{1}{n}\ln(C_e) \tag{9}$$

where q_t and q_e are the concentration of the metals sorbed onto the WTR granules at time t and equilibrium, respectively. K_L is Langmuir isotherm constant, Q^0_{max} is maximum saturated monolayer adsorption capacity of an adsorbent, K_F is Freundlich isotherm capacity parameter and 1/n is Freundlich isotherm intensity parameter. In addition, separation factor (R_L) (Hall et al., 1966), which is derived from K_L as shown in Eq. (10), was also determined
The separation factor (R_L):

$$R_L = \frac{1}{1 + K_L C_0} \tag{10}$$

In contrast to the Langmuir and Freundlich models, the surface complexation model (SCM) allows the prediction of the sorption processes at solid-water interfaces by considering the impact of solution chemistry, such as pH and ionic strength. This is important for predicting the removal performance before implementing the WTR granule-based stormwater treatment systems particularly because stormwater is known to have a high variation in water chemistry from both

temporal and spatial aspects. Based on the data from the sorption edge study, surface complexation modeling was performed using MINEQL+ version 5.0 (Environmental Research Software, ME, USA) in conjunction with MINFIT (Xie et al., 2016). A triple-layer model (TLM) was used for this study. The TLM considers the solid-water interfaces into three regions: (1) a surface plane for strongly adsorbed ions including H^+ and OH^-, (2) a near-surface plane for weakly adsorbed ions, (3) a diffused layer plane. Compared to the other models (e.g., constant capacitance and diffuse layer models), the TLM provides an advantage to take the influence of the electrolyte ions into account (Wen et al., 1998).

2.9. Chemical and statistical analysis

Certified reference solutions were analyzed along with the samples. Both internal and external standards were analyzed in all ICP-OES analyses. The calibration was performed before each analysis with an R^2 greater than 0.995. Triplicate measurements were performed for each sample. The ICP Expert Software (Agilent Technologies, CA, USA) was used to operate and process the ICP-OES data. The containers used in all experiments were cleaned with laboratory-grade detergent, soaked in 10% nitric acid solution overnight, soaked in DI water, and rinsed with DI water. All studies were performed in triplicate. The Tukey–Kramer HSD (honestly significant difference) test was performed to determine significant differences ($p < 0.05$) using the JMP statistical software package (JMP 15.2, SAS Institute Inc., NC, USA).

3. Results and discussion

3.1. Characterization

3.1.1. SEM-EDS

SEM was used to investigate the surface morphology and changes in the WTR granules. The results are shown in Fig. 1. The WTR granules form a 3D network of cross-linked calcium alginate retaining the WTR. The EDS spectrum in Figure S1 reveals the major components of the WTR granules: Al, C, O, and Si; along with the exchangeable cations (Mg^{2+}, Ca^{2+}, K^+). The SEM image (Fig. 1b) reveals the presence of macropores in the WTR granules. After sorption, no significant changes were observed (Fig. 1a and b), showing that the surface and structural integrity of the WTR granules were not affected by exposure to heavy metals in aqueous solutions. The elemental mapping images show the distribution of Cd, Cr, and Ni within the WTR granules (Fig. 1e, 1f, and 1g). The concentration gradient of the adsorbed heavy metal was pronounced after sorption with Cr (Fig. 1f) suggesting intraparticle diffusion.

3.1.2. FTIR

The FTIR spectra of the milled WTR (before granulation), fresh WTR granules, and treated WTR granules with the three heavy metals are presented in Fig. 2. There were broad vibrational bands around 3440 cm^{-1} attributed to the O–H stretching (Antunes Boca Santa et al., 2013). Mineral functional groups were detected on the surface, including Al–OH at 1032 cm^{-1} (Jiao et al., 2017), Si–O–T (T is tetrahedral Si or Al) at 778, and 470 cm^{-1} (Flanigen et al., 1974; Ji et al., 2020), and Al-O at 534 cm^{-1} (Rajapaksha et al., 2012) which is consistent with the SEM-EDS results.

The bands that occurred at 1627–1640 cm^{-1} indicate H_2O bending vibrations (Frost et al., 2001; Li et al., 2009). The peaks at 797 cm^{-1} and 694 cm^{-1} indicate OH deformation and translation, respectively (Frost et al., 2001). The peaks between 1385 and 1422 cm^{-1} are attributed to –COO– symmetrical stretching vibrations (Papageorgiou et al., 2010). No substantial change was observed between the milled WTR (before granulation) and fresh WTR granules, suggesting that the granulation process did not inhibit or remove the functional groups of the WTR. The peak at 1412 cm^{-1} (–COO– symmetrical stretching vibrations) of the milled WTR blue-shifted to 1422 cm^{-1} after the granulation process indicating the formation of crossed-linked calcium alginate. After being exposed to the three metals, this peak shifted to lower wavenumbers (1419 cm^{-1}), and the bands at 1385 cm^{-1} were observed in the presence of cadmium and nickel, suggesting the interaction of the COO functional groups with the added metals. The increase in intensity of the bands at about 1385 cm^{-1} after being loaded with metals is consistent with the findings of Zhao et al. (2011) who suggested that these changes may be associated with the adsorption of metals. The peak intensity at 1083 cm^{-1} was enhanced after being loaded with metals, suggesting the interaction of the –OH groups with the three metals (Huang et al., 2009).

3.2. Kinetic study

The effect of contact time on Cd, Cr, and Ni removal by WTR granules is shown in Fig. 3. The WTR granules were capable of removing Cd, Cr, and Ni simultaneously. Within the first 2 h, more than 60% of Cd and Cr were removed, while almost 40% removal of Ni was achieved. More than 83%, 91%, and 59% removal of Cd, Cr, and Ni were achieved after 36 h.

The fast removal observed in the first stage of the experiment was potentially due to the sorption processes that occur at the solid-solution interface of the outer surface of the sorbent, which was readily accessible. Generally, the sorption processes onto porous materials like the WTR granules are expected to take a longer time compared to nonporous adsorbents, especially after the first 2 h. This is mainly due to the different sorption mechanisms of the sorbents. For the porous materials, pore filling is the most common sorption mechanism that occurs in addition to other mechanisms (e.g., cation exchange, surface precipitation, and electrostatic attraction) (Tran et al., 2017).

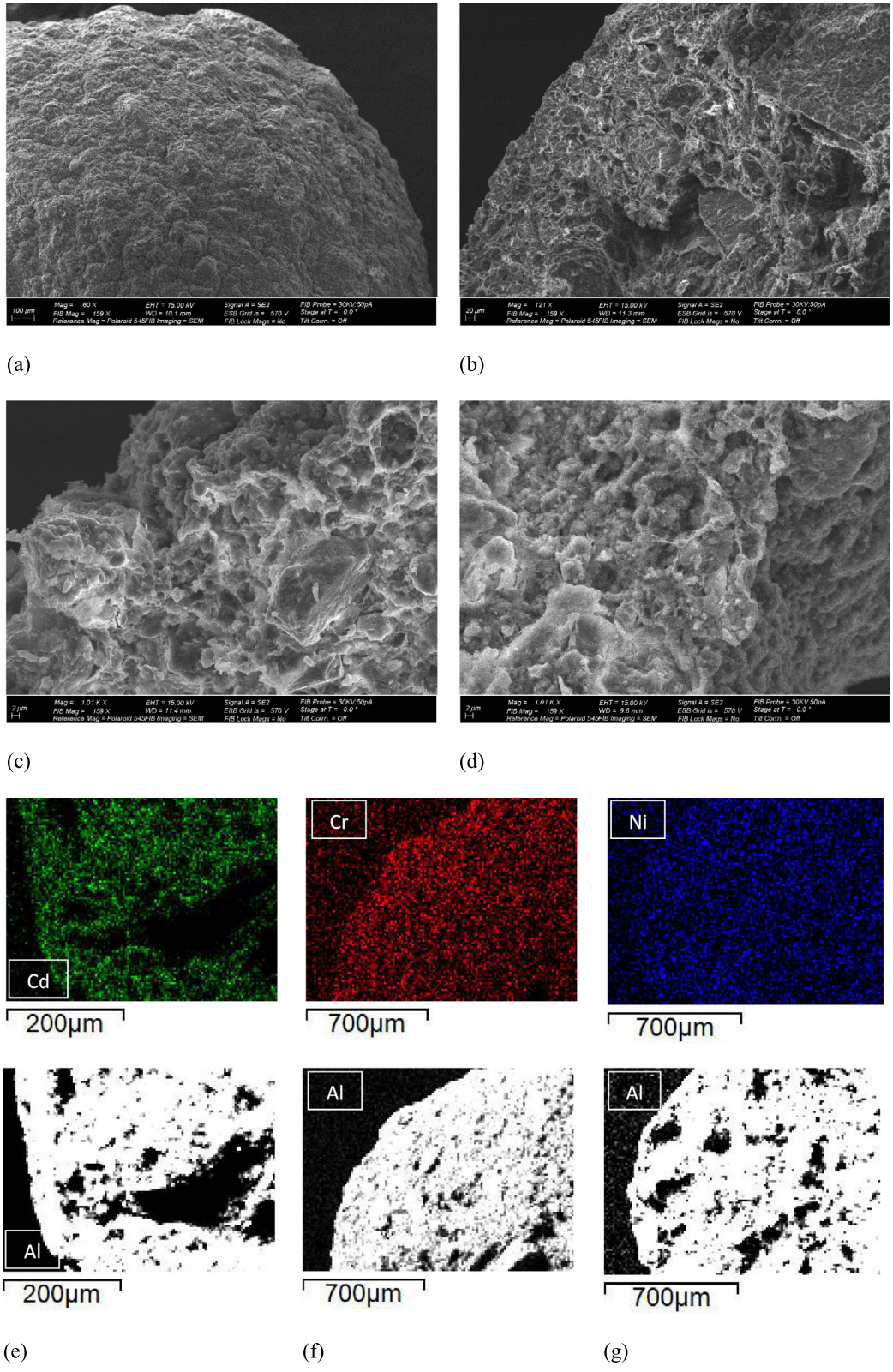

Fig. 1. SEM images of WTR granules (a) surface, (b) cross-section, (c) before sorption, (d) after sorption; and elemental mapping images of the WTR granule cross-section after sorption with (e) Cd, (f) Cr, and (g) Ni.

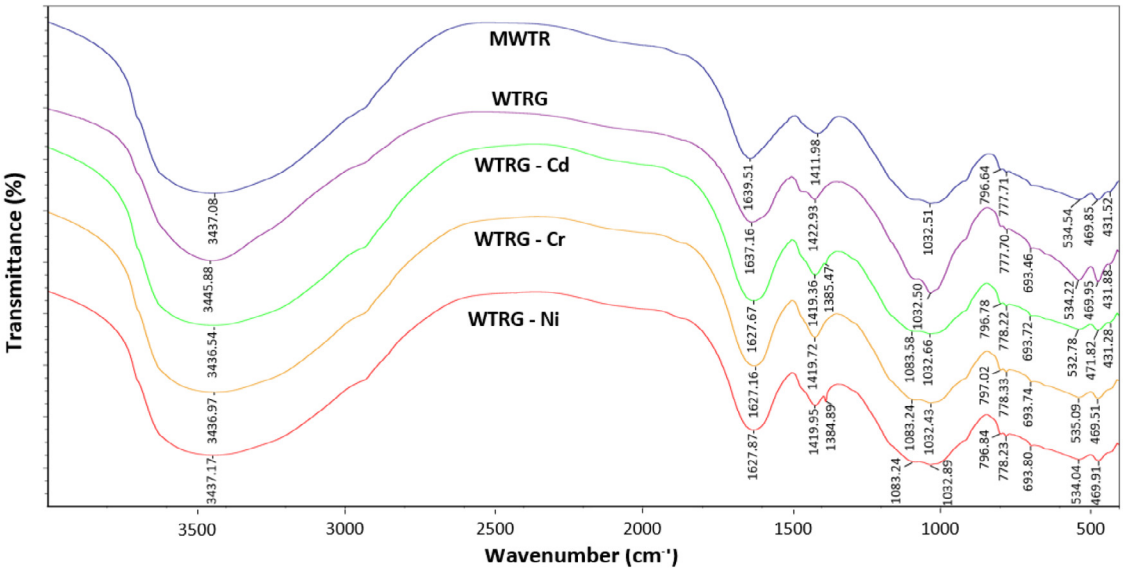

Fig. 2. FTIR transmittance spectra of milled WTR (MWTR), fresh WTR granules (WTRG), WTR granules after treated with Cd (WTRG-Cd), Cr (WTRG-Cr), and Ni (WTRG-Ni)..

The fitted PFO, PSO, and intraparticle diffusion model parameters are shown in Table S1. For all three heavy metals, the experimental data were fitted very well by the PSO model ($R^2 > 0.99$). In addition, the q_e values calculated from the PSO model were more comparable to the q_e values from the experiment, further indicating the PSO model provided the best fit for the experimental kinetic data.

While the PSO model is capable of accurately describing sorption kinetic experimental data, it does not reveal the sorption mechanisms (Tran et al., 2017). The intra-particle diffusion model, on the other hand, can be used to identify sorption processes, as well as predict the rate-controlling step. To identify if the sorption is controlled by intra-particle diffusion, a plot of q_t against $t^{0.5}$ is presented in Fig. 3b. In general, if the intra-particle diffusion plot is linear and passes through the origin, the sorption is entirely governed by intra-particle diffusion (Tran et al., 2017). In this study, the overall experimental data were not fit well ($R^2 < 0.79$) by the intra-particle diffusion model (Table S1). Instead, the biphasic relationship was observed in all three heavy metals. This indicated that intra-particle diffusion was the rate-controlling step only in the first 2 h. The overall sorption process was controlled by a multistep mechanism.

3.3. Sorption isotherm study

The experimental data of each target metal pollutant from the sorption isotherm study are presented in Fig. 4. The Langmuir and Freundlich isotherm parameters of Cd, Cr, and Ni are presented in Table S2. Both Langmuir and Freundlich isotherm models provide excellent fits of the isotherm data of Cd, Cr, and Ni ($R^2 > 0.98$). Langmuir isotherm gave a marginally better fit for Ni sorption ($R^2 > 0.99$), while Freundlich isotherm better represented Cd sorption ($R^2 > 0.99$). The Langmuir sorption capacity ($Q^0{}_{max}$) was in the order of Cd > Cr > Ni. The values of K_L and K_F are in the same order of Cr > Cd > Ni. To identify if the sorption is favorable, separation factor (R_L) and Freundlich exponent (n) were considered. The sorption is considered favorable when the values of R_L and n are less than 1 (Tran et al., 2017). Based on the results as shown in Table S2, sorption of Cd, Cr, and Ni on the WTR granules is considered favorable.

Table S3 shows the sorption capacity ($Q^0{}_{max}$) of the WTR granules in comparison to various filter materials for metal removal from stormwater runoff. The WTR granules had substantially higher Cd and Cr sorption capacities compared to calcite, zeolite, sand, and iron filing. The Ni sorption capacity of WTR granules was comparable with calcite but lower than zeolite and iron filings (Reddy et al., 2014). WTR granules showed higher Cd, Cr, and Ni sorption capacities compared to all 11 filter materials used in stormwater bioretention facilities reported in Søberg et al. (2019).

3.4. Effect of environmental parameters

3.4.1. Effect of background electrolyte on Cd, Cr, and Ni removal

Four cations, including two monovalent (Na^+ and K^+) and two divalent cations (Ca^{2+} and Mg^{2+}), and two anions (Cl^- and $NO_3{}^-$) were used to investigate the effect of background electrolytes on Cd, Cr, and Ni removal (Fig. 5a). The effect of background anions was examined by comparing the results between NaCl and $NaNO_3$. Background anions had a significant effect ($p < 0.05$) only on Cd removal, while no significant difference was observed in the case of Cr and Ni

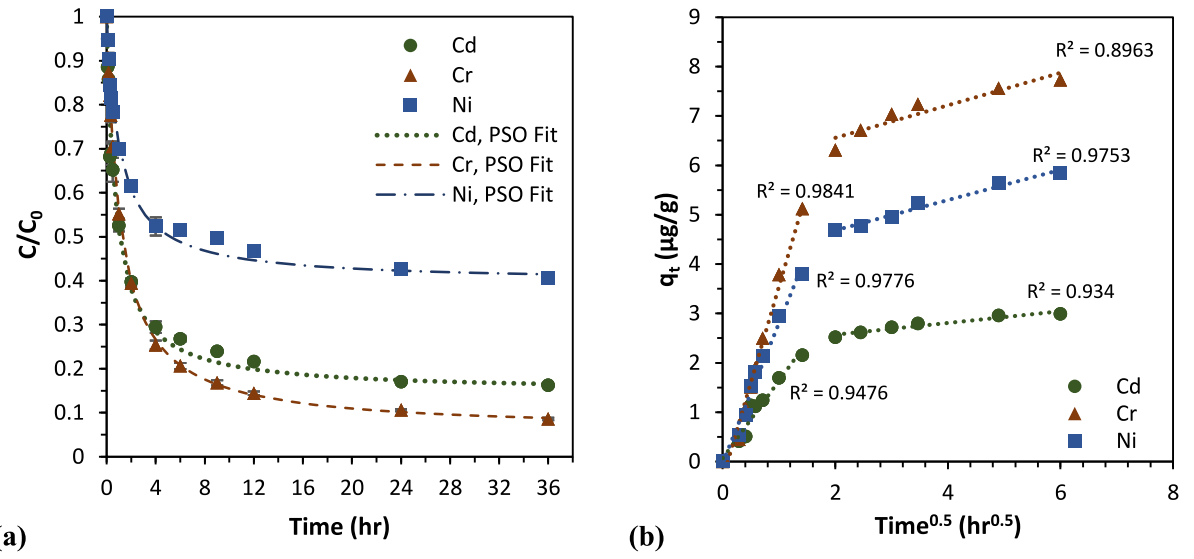

Fig. 3. Effect of contact time on Cd, Cr, and Ni removal by WTR granules showing (a) the relationship between C/C_0 and time and (b) the amount of heavy metals adsorbed by the WTR granules and time$^{0.5}$. Symbols represent experimental data and lines are fitting curves of (a) the pseudo-second-order model and (b) linear regression. (WTR granules = 10 g/L; pH = 7.0; initial concentrations: Cd = 35 mg/L, Cr = 85 mg/L, Ni = 100 mg/L; ionic strength = 0.1 M $NaNO_3$; T = 23 °C).

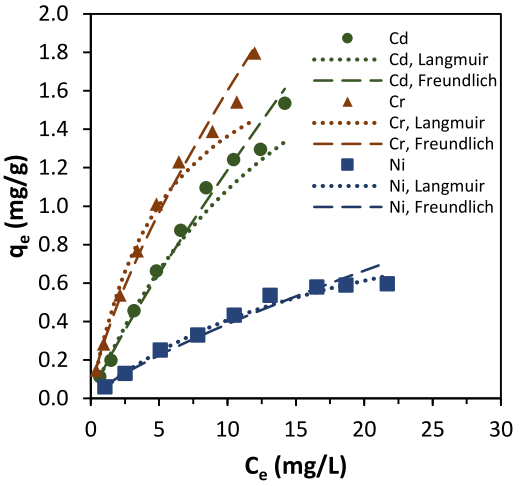

Fig. 4. Langmuir and Freundlich isotherms of Cd, Cr, and Ni on the WTR granules. Symbols represent experimental data and lines are fitting curves of the Langmuir and Freundlich isotherm models. (WTR granules = 10 g/L; pH = 7.0; ionic strength = 0.1 M $NaNO_3$; T = 23 °C).

removal. This was potentially because Cd ions could form water-soluble complexes with Cl^- and NO_3^- (e.g., $CdCl^+$ and $CdNO_3^+$), which led to the lower electrostatic attraction between the Cd ions and the surface of the WTR granules. The lower Cd removal was observed with the presence of Cl^- compared to NO_3^- which was primarily because of the higher tendency of Cl^- to complex Cd ions (Hu et al., 2014). The distribution of the Cd species calculated using MINEQL+ Version 5 is presented in Figure S2, showing that the proportion of the Cd^{2+} ions is drastically lower in the presence of Cl^- ions (~19%) compared to NO_3^- ions (~90%). The removal of Cd, as shown in Fig. 5b, was similar to the proportion of the Cd^{2+} ions in the case of $NaNO_3$. Interestingly, the removal of Cd in the case of NaCl exceeded the proportion of the Cd^{2+} ions. This finding suggests that $CdCl^+$ has a higher tendency to be removed compared to $CdNO_3^+$. The influence of both Cl^- and NO_3^- on Ni and Cr removal was found to be comparable.

The influences of the background electrolyte cations on the removal of all three heavy metals were in the following sequence: $CaCl_2 > MgCl_2 > KCl \sim NaCl$. The divalent cations ($Ca^{2+}$ and Mg^{2+}) had a significantly greater ($p < 0.05$) adverse influence on the Cd, Cr, and Ni removal than the monovalent cations (K^+ and Na^+). This was potentially due to the higher concentration of Cl^- which was double in the case of the divalent cations compared to the monovalent cations. The higher concentration of Cl^- could induce more water-soluble complex of the heavy metals as detailed previously, resulting in

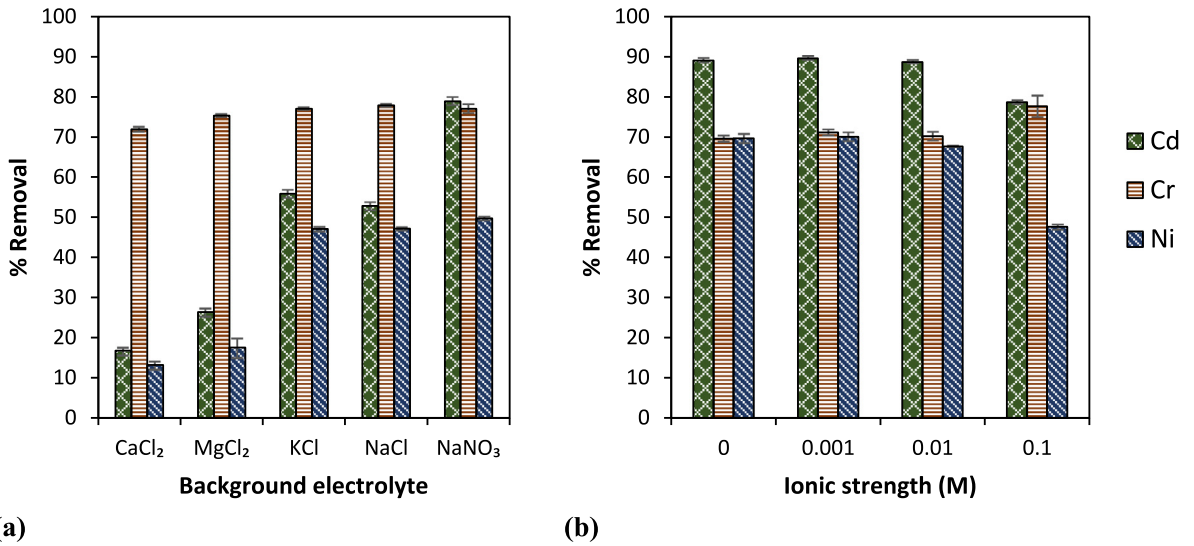

Fig. 5. Effects of (a) background electrolyte and (b) ionic strength on the removal of Cd, Cr, and Ni onto the WTR granules. (WTR granules = 10 g/L; pH = 7.0; initial concentrations of Cd, Cr, and Ni = 5 mg/L; T = 23 °C).

the reduction in removal by more than half of the removal with the presence of monovalent cations. However, the higher concentration of Cl^- was not the sole reason for the decrease in removal since the difference between the divalent cations (Ca^{2+} and Mg^{2+}) was also observed. The inhibitory influence of divalent cations on the removal of heavy metals was in the order of $Ca^{2+} > Mg^{2+}$. The findings were consistent with the previous study by Hu et al. (2014) in which the adsorption of Cd onto magnetic graphene oxide-supported sulfanilic acid (MGO-SA) was examined. The recent study by Esfandiar et al. (2022) also indicated that the inhibitory effect of divalent cations on the removal of metals was stronger than that of monovalent cations. The influence of the electrolytes was the most pronounced in the removal of Cd, followed by Ni and Cr, respectively.

3.4.2. Effect of ionic strength on Cd, Cr, and Ni removal

The ionic strength of an aqueous matrix is a very important parameter that affects the adsorption of heavy metal ions at the solid–liquid interface (Stumm, 1992). The effects of ionic strength on the removal of Cd, Cr, and Ni onto the WTR granules are shown in Fig. 5b. The increases in the ionic strength from 0 to 0.1 M resulted in a decrease in the removal of Cd and Ni, which were present in the solution as cations. The removal of Cd and Ni at an ionic strength of 0.1 M significantly decreased ($p < 0.05$) compared to the lower ionic strength. These results are in line with the previous studies (Hu et al., 2014; Jiang et al., 2010; Rajapaksha et al., 2012; Reed and Nonavinakere, 1992; Wang et al., 2007). However, the change was observed only when the ionic strength was higher than 0.01 M. When the ionic strength increased, more positively charged Na ions potentially hindered the Cd and Ni access to available sorption sites on the WTR granules (Reed and Nonavinakere, 1992). On the other hand, the trend was opposite in the case of Cr, which was present in the solution as anions including CrO_4^{2-}, $HCrO_4^-$ and $Cr_2O_7^{2-}$ (Li et al., 2009). The removal of Cr at an ionic strength of 0.1 M was significantly greater ($p < 0.05$) than the lower ionic strength. Generally, the background electrolytes are present in the same plane as outer-sphere complexes. As a result, outer-sphere complexes are more sensitive to the change in ionic strength compared to inner-sphere complexes. The decreasing adsorption with increasing solution ionic strength could indicate that outer-sphere complexes are formed, or a mixture of inner-sphere and outer-sphere complexes is formed. In contrast, no ionic strength dependence or increasing adsorption with increasing solution ionic strength is indicative of an inner-sphere adsorption mechanism (Goldberg et al., 2001, 2007). Therefore, the adsorption of Cr could be attributed to inner-sphere complexation. The adverse dependence on ionic strength adsorption of Cd and Ni suggested that the sorption of Cd and Ni potentially involves outer-sphere complexation.

3.5. Sorption edge study and surface complexation modeling

Metal-ion sorption is pH-dependent due to the influence of pH on the surface properties of the adsorbent, and the ionic forms of the heavy metals in solution (Ajouyed et al., 2010; Tran et al., 2017). Therefore, it is critical to examine the sorption characteristics of Cd, Cr, and Ni onto the WTR granules under different pH. In this study, the pH range of 5.5 to 8 was selected based on the typical pH range of the stormwater runoff (Göbel et al., 2007). The effect of pH on the sorption of Cd, Cr, and Ni onto the WTR granules is presented in Fig. 6. Two different heavy metal removal responses to pH variation were observed. The removal of Cd and Ni was favorable when pH was more than 6.5. In contrast, the removal

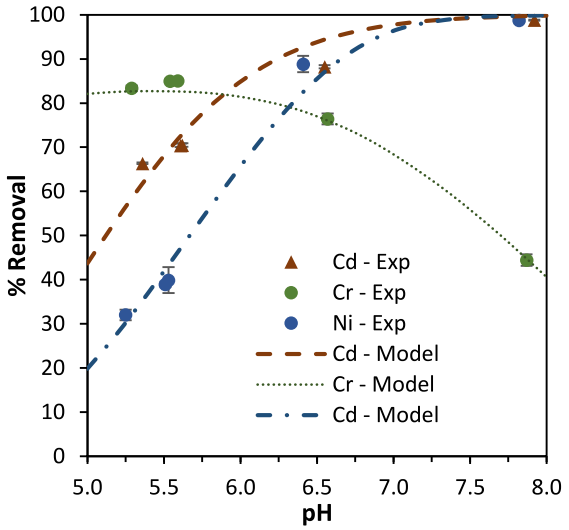

Fig. 6. Effect of pH on the sorption of Cd, Cr, and Ni onto the WTR granules. Symbols represent experimental data and lines are fitting curves of the surface complexation model. (WTR granules = 10 g/L; initial concentrations of Cd, Cr, and Ni = 5 mg/L; ionic strength = 0.1 M $NaNO_3$; T = 23 °C).

of Cr in which the removal decreased substantially when the pH was more than 6.5. This strong effect of pH is closely related to the speciation of heavy metal ions and the charge of the WTR granule surfaces. At low pH, the WTR granule surface was positively charged. Therefore, the WTR granule surface was attractive to the Cr ions, which were negatively charged, resulting in favorable removal of Cr. However, at such pH level, a repulsive electrostatic force was produced between positively charged ions (i.e., Cd and Ni ions) and the positively charged surface, resulting in unfavorable removal of Cd and Ni.

Based on the SEM-EDS results, Al and O were found to be two major elements on the surface of the WTR granules suggesting that aluminum hydroxide (AlOH) can be considered as the primary sites, which are in line with the previous studies (Nagar et al., 2010; Punamiya et al., 2013). The surface reactions of AlOH consist of protonation and deprotonation, which are shown in Table 1. Generally, Cd, Cr, and Ni can be described by inner- or outer-sphere complexations. Examples of possible reaction stoichiometries can be expressed as follows:
Inner-sphere complexation:

$$\equiv AlOH + Cd^{+2} = \equiv AlOCd^{+} + H^{+}$$
$$\equiv AlOH + CrO_4{}^{-2} + H^{+} = \equiv AlCrO4^{-2} + H_2O$$
$$\equiv AlOH + Ni^{+2} = \equiv AlONi^{+} + H^{+}$$

Outer-sphere complexation:

$$\equiv AlOH + Cd^{+2} + H_2O = \equiv AlOCdOH + 2H^{+}$$
$$\equiv AlOH + H^{+} + CrO_4{}^{-2} = \equiv AlOH_2{}^{+}...CrO_4{}^{2-}$$
$$\equiv AlOH + Ni^{+2} + H_2O = \equiv AlOCdOH + 2H^{+}$$

Previous studies showed that Cd and Ni removal by metal oxides was governed by an inner-sphere monodentate bonding mechanism (Manceau et al., 2000; Rajapaksha et al., 2012). Based on the sorption edge study, the profile of the Cr removal in exhibited a convex curve with a peak at pH 5.5, suggesting the dominance of monodentate complexes (Johnston and Chrysochoou, 2014). In addition, the coordinating environment of sorbed As, an oxyanion similar to Cr, on WTR has been reported to be inner-sphere complexation (Makris et al., 2007, 2009). Therefore, inner-sphere monodentate complexation was considered in this study. The surface complexation reactions for Cd, Cr, and Ni are shown in Table 1. The parameters for surface complexation models are shown in Table 2.

Experimental data for Cr and Ni are very well described by the surface complexation models, but adsorption of Ni is underpredicted at pH∼6.5. In the case of Cd adsorption, the model is overpredicted at pH∼6.5. Overall, the surface complexation models can predict the adsorption of Cd, Cr, and Ni. The intrinsic complexation constants of Cd, Cr, and Ni in Table 1 show that the affinity of the three heavy metals with the WTR granules is in the order of Cr > Cd > Ni.

It is worth noting that the capacitance values and protonation and deprotonation reaction constants were taken from a previous study (Goldberg et al., 2001). These parameters can be affected by crystallinity or morphology, which are unique for each material (Reich and Koretsky, 2011). Therefore, the parameters used in this model may not be fully representative

Table 1
Surface reactions and surface complexation reactions.

Reaction	logK	References
Surface reaction		
$\equiv AlOH = \equiv AlO^- + H^+$	−11.2	Goldberg et al. (2001)
$\equiv AlOH + H^+ = \equiv AlOH_2{}^+$	5.0	Goldberg et al. (2001)
Surface complexation reactions		
$\equiv AlOH + Cd^{+2} = \equiv AlOCd^+ + H^+$	−0.20	This study
$\equiv AlOH + CrO_4{}^{-2} + H^+ = \equiv AlCrO4^{-2} + H_2O$	15.88	This study
$\equiv AlOH + Ni^{+2} = \equiv AlONi^+ + H^+$	−2.23	This study

Table 2
WTR granules and solution properties used in the surface complexation modeling.

Parameter	Value
Surface area (m^2/g)	24.12
Total surface sites (mol L^{-1})	3×10^{-4}
C_1 (F m^{-2})[a]	1.2
C_2 (F m^{-2})[a]	0.2
Initial concentration (mg L^{-1})	5
Ionic strength (M, $NaNO_3$)	0.1

[a]Goldberg et al. (2001)

of the crystallinity or morphology of the WTR granules. In addition, only inner-sphere monodentate complexation was considered in these models; outer-sphere and multidentate complexations were not included. The accuracy of the models can be further improved by integrating multiple complexes or multiple site models.

4. Practical applications and future research prospects

The findings from this study have important implications for the design of stormwater treatment systems using the WTR granules. It is essential to examine the kinetic and sorption isotherm data before implementing a new treatment system. A longer reaction time would lead to lower metal concentrations in stormwater. Treatment system designs that increase residence time, such as baffles in the treatment channel or a greater bed depth, can be utilized to promote metal removal. Together with the expected metal amount in the target treatment areas, the results from sorption isotherm studies can be used to determine the quantity of the WTR granules needed for the implementation of the treatment system, and estimate their service lifetime. Electrolytes in the target treatment areas may be considered to determine the potential inhibiting or enhancing effects on the metal removal. The surface complexation models and intrinsic complexation constants obtained can be used to predict the removal performance under different water chemistry. The results from this study provide essential insights into the potential of WTR granules for the successful treatment of stormwater runoff. The effect of co-contaminants and humic acid, long-term removal under flow-through conditions, and the removal performance with real stormwater runoff under field conditions, remains to be further investigated to gain a better understanding of the performance capacity of this green and innovative sorbent.

5. Conclusions

The WTR granules simultaneously removed Cd, Cr, and Ni. The pseudo-second-order, Langmuir, and Freundlich models adequately explained the removal characteristics of all three heavy metals. Environmental parameters had different effects on the metal removal by the WTR granules. At > 0.01 M ionic strength, Cd and Ni adsorption decreased, whereas sorption of Cr increased as ionic strength increased. Anions in the background electrolyte had a strong effect on Cd sorption. Divalent cations had a greater negative impact on metal removal than monovalent cations. Surface complexation modeling suggested that adsorption of Cr was mainly governed by inner-sphere complexation, while the sorption of Cd and Ni also involved outer-sphere complexation. The TLM model adequately described the removal of Cd, Cr, and Ni in a typical pH range of stormwater runoff. The WTR granules can be readily implemented as green filter media to remove heavy metals from stormwater runoff.

CRediT authorship contribution statement

Viravid Na Nagara: Methodology, Data collection and analysis, Writing - original draft. **Dibyendu Sarkar:** Conceptualization, Supervision, Funding acquisition, Project management, Writing - review & editing. **Evert J. Elzinga:** Data collection, Data curation, Writing - review & editing. **Rupali Datta:** Writing - review & editing.

Declaration of competing interest

The authors declare the following financial interests/personal relationships which may be considered as potential competing interests: Dibyendu Sarkar has patent pending to The Trustees of the Stevens Institute of Technology, Hoboken, NJ (US).

Acknowledgments

This publication is the result of research sponsored by the New Jersey Sea Grant Consortium (NJSGC) with funds from the National Oceanic and Atmospheric Administration (NOAA), Office of Sea Grant, U.S. Department of Commerce, under NOAA grant number NA10OAR4170075 and the NJSGC. The statements, findings, conclusions, and recommendations are those of the author(s) and do not necessarily reflect the views of the NJSGC or the U.S. Department of Commerce (NJSG-22-981). The authors would like to acknowledge Dr. Tsengming Chou from The Laboratory for Multiscale Imaging (LMSI) at SIT for providing technical support during the SEM-EDS analysis and the New Jersey American Water (NJAW) Water Treatment Plant in Bridgewater Township, NJ for providing WTR. The technical assistance of undergraduate student Caitlin Carroll is gratefully acknowledged. The authors would like to thank Sameer Neve for his assistance in the surface area and FTIR analyses.

Appendix A. Supplementary data

Supplementary material related to this article can be found online at https://doi.org/10.1016/j.eti.2022.102636.

References

Ajouyed, O., Hurel, C., Ammari, M., Allal, L. Ben, Marmier, N., 2010. Sorption of Cr(VI) onto natural iron and aluminum (oxy)hydroxides: Effects of pH, ionic strength and initial concentration. J. Hazard. Mater. 174, 616–622. http://dx.doi.org/10.1016/J.JHAZMAT.2009.09.096.

Alam, M.Z., Anwar, A.H.M.F., Heitz, A., Sarker, D.C., 2018. Improving stormwater quality at source using catch basin inserts. J. Environ. Manage. 228, 393–404. http://dx.doi.org/10.1016/j.jenvman.2018.08.070.

Antunes Boca Santa, R.A., Bernardin, A.M., Riella, H.G., Kuhnen, N.C., 2013. Geopolymer synthetized from bottom coal ash and calcined paper sludge. J. Clean. Prod. 57, 302–307. http://dx.doi.org/10.1016/J.JCLEPRO.2013.05.017.

Blanchard, G., Maunaye, M., Martin, G., 1984. Removal of heavy metals from waters by means of natural zeolites. Water Res. 18, 1501–1507. http://dx.doi.org/10.1016/0043-1354(84)90124-6.

Castaldi, P., Silvetti, M., Garau, G., Demurtas, D., Deiana, S., 2015. Copper(II) and lead(II) removal from aqueous solution by water treatment residues. J. Hazard. Mater. 283, 140–147. http://dx.doi.org/10.1016/j.jhazmat.2014.09.019.

Cederkvist, K., Ingvertsen, S.T., Jensen, M.B., Holm, P.E., 2013. Behaviour of chromium(VI) in stormwater soil infiltration systems. Appl. Geochem. 35, 44–50. http://dx.doi.org/10.1016/J.APGEOCHEM.2013.05.011.

Chakraborty, R., Asthana, A., Singh, A.K., Jain, B., Susan, A.B.H., 2020. Adsorption of heavy metal ions by various low-cost adsorbents: a review. Int. J. Environ. Anal. Chem. 1–38.

Duan, R., Fedler, C.B., 2021. Adsorptive removal of Pb2+ and Cu2+ from stormwater by using water treatment residuals. Urban Water J. 18, 237–247. http://dx.doi.org/10.1080/1573062X.2021.1877742.

Esfandiar, N., Suri, R., McKenzie, E.R., 2022. Competitive sorption of Cd, Cr, Cu, Ni, Pb and Zn from stormwater runoff by five low-cost sorbents; effects of co-contaminants, humic acid, salinity and pH. J. Hazard. Mater. 423, 126938. http://dx.doi.org/10.1016/J.JHAZMAT.2021.126938.

Flanagan, K., Branchu, P., Boudahmane, L., Caupos, E., Demare, D., Deshayes, S., Dubois, P., Meffray, L., Partibane, C., Saad, M., Gromaire, M.C., 2019. Retention and transport processes of particulate and dissolved micropollutants in stormwater biofilters treating road runoff. Sci. Total Environ. 656, 1178–1190. http://dx.doi.org/10.1016/J.SCITOTENV.2018.11.304.

Flanigen, E.M., Khatami, H., Szymanski, H.A., 1974. Infrared structural studies of zeolite frameworks. In: Molecular Sieve Zeolites-I. In: Advances in Chemistry, AMERICAN CHEMICAL SOCIETY, pp. 16–201. http://dx.doi.org/10.1021/ba-1971-0101.ch016.

Freundlich, H., 1907. Über die adsorption in lösungen. Z. Phys. Chem. 57, 385–470.

Frost, R.L., Locos, O.B., Ruan, H., Kloprogge, J.T., 2001. Near-infrared and mid-infrared spectroscopic study of sepiolites and palygorskites. Vib. Spectrosc. 27, 1–13. http://dx.doi.org/10.1016/S0924-2031(01)00110-2.

Göbel, P., Dierkes, C., Coldewey, W.G., 2007. Storm water runoff concentration matrix for urban areas. J. Contam. Hydrol. 91, 26–42.

Goldberg, S., Criscenti, L.J., Turner, D.R., Davis, J.A., Cantrell, K.J., 2007. Adsorption–desorption processes in subsurface reactive transport modeling. Vadose Zo. J. 6, 407–435.

Goldberg, S., Johnston, C.T., Brown, G.E., 2001. Mechanisms of arsenic adsorption on amorphous oxides evaluated using macroscopic measurements, vibrational spectroscopy, and surface complexation modeling. J. Colloid Interface Sci. 234, 204–216. http://dx.doi.org/10.1006/jcis.2000.7295.

Hall, K.R., Eagleton, L.C., Acrivos, A., Vermeulen, T., 1966. Pore- and solid-diffusion kinetics in fixed-bed adsorption under constant-pattern conditions. Ind. Eng. Chem. Fundam. 5, 212–223. http://dx.doi.org/10.1021/i160018a011.

Hu, Xin jiang, Liu, Y. guo, Zeng, G. ming, You, S. hong, Wang, H., Hu, Xi, Guo, Y. ming, Tan, X. fei, Guo, F. ying, 2014. Effects of background electrolytes and ionic strength on enrichment of Cd(II) ions with magnetic graphene oxide-supported sulfanilic acid. J. Colloid Interface Sci. 435, 138–144. http://dx.doi.org/10.1016/j.jcis.2014.08.054.

Hu, Y.S., Zhao, Y.Q., Zhao, X.H., Kumar, J.L.G., 2012. Comprehensive analysis of step-feeding strategy to enhance biological nitrogen removal in alum sludge-based tidal flow constructed wetlands. Bioresour. Technol. 111, 27–35. http://dx.doi.org/10.1016/J.BIORTECH.2012.01.165.

Huang, G., Zhang, H., Shi, J.X., Langrish, T.A.G., 2009. Adsorption of chromium(VI) from aqueous solutions using cross-linked magnetic chitosan beads. Ind. Eng. Chem. Res. 48, 2646–2651. http://dx.doi.org/10.1021/ie800814h.

Huber, M., Welker, A., Helmreich, B., 2016. Critical review of heavy metal pollution of traffic area runoff: Occurrence, influencing factors, and partitioning. Sci. Total Environ. 541, 895–919. http://dx.doi.org/10.1016/j.scitotenv.2015.09.033.

Ji, Z., Su, L., Pei, Y., 2020. Synthesis and toxic metals (Cd, Pb, and Zn) immobilization properties of drinking water treatment residuals and metakaolin-based geopolymers. Mater. Chem. Phys. 242, 122535. http://dx.doi.org/10.1016/J.MATCHEMPHYS.2019.122535.

Jiang, M. qin, Jin, X. ying, Lu, X.Q., Chen, Z. liang, 2010. Adsorption of Pb(II), Cd(II), Ni(II) and Cu(II) onto natural kaolinite clay. Desalination 252, 33–39. http://dx.doi.org/10.1016/J.DESAL.2009.11.005.

Jiao, J., Zhao, J., Pei, Y., 2017. Adsorption of Co(II) from aqueous solutions by water treatment residuals. J. Environ. Sci. 52, 232–239. http://dx.doi.org/10.1016/J.JES.2016.04.012.
Johnston, C.P., Chrysochoou, M., 2014. Mechanisms of chromate adsorption on hematite. Geochim. Cosmochim. Acta 138, 146–157. http://dx.doi.org/10.1016/J.GCA.2014.04.030.
Kumar, P.S., Korving, L., van Loosdrecht, M.C.M., Witkamp, G.J., 2019. Adsorption as a technology to achieve ultra-low concentrations of phosphate: Research gaps and economic analysis. Water Res. X 4, 100029. http://dx.doi.org/10.1016/J.WROA.2019.100029.
Lagergren, S.K., 1898. About the theory of so-called adsorption of soluble substances. Sven. Vetenskapsakad. Handingarl 24, 1–39.
Lange, K., Österlund, H., Viklander, M., Blecken, G.T., 2020. Metal speciation in stormwater bioretention: Removal of particulate, colloidal and truly dissolved metals. Sci. Total Environ. 724. http://dx.doi.org/10.1016/j.scitotenv.2020.138121.
Langmuir, I., 1918. The adsorption of gases on plane surfaces of glass, mica and platinum. J. Am. Chem. Soc. 40, 1361–1403.
Li, Y., Gao, B., Wu, T., Sun, D., Li, X., Wang, B., Lu, F., 2009. Hexavalent chromium removal from aqueous solution by adsorption on aluminum magnesium mixed hydroxide. Water Res. 43, 3067–3075. http://dx.doi.org/10.1016/J.WATRES.2009.04.008.
Liu, J., Davis, A.P., 2014. Phosphorus speciation and treatment using enhanced phosphorus removal bioretention. Environ. Sci. Technol. 48, 607–614. http://dx.doi.org/10.1021/es404022b.
Makris, K.C., Harris, W.G., O'Connor, G.A., Obreza, T.A., Elliott, H.A., 2005. Physicochemical properties related to long-term phosphorus retention by drinking-water treatment residuals. Environ. Sci. Technol. 39, 4280–4289. http://dx.doi.org/10.1021/es0480769.
Makris, K.C., Sarkar, D., Datta, R., 2006. Aluminum-based drinking-water treatment residuals: A novel sorbent for perchlorate removal. Environ. Pollut. 140, 9–12. http://dx.doi.org/10.1016/j.envpol.2005.08.075.
Makris, K.C., Sarkar, D., Parsons, J.G., Datta, R., Gardea-Torresdey, J.L., 2007. Surface arsenic speciation of a drinking-water treatment residual using X-ray absorption spectroscopy. J. Colloid Interface Sci. 311, 544–550. http://dx.doi.org/10.1016/J.JCIS.2007.02.078.
Makris, K.C., Sarkar, D., Parsons, J.G., Datta, R., Gardea-Torresdey, J.L., 2009. X-ray absorption spectroscopy as a tool investigating arsenic(III) and arsenic(V) sorption by an aluminum-based drinking-water treatment residual. J. Hazard. Mater. 171, 980–986. http://dx.doi.org/10.1016/J.JHAZMAT.2009.06.102.
Manceau, A., Nagy, K.L., Spadini, L., Ragnarsdottir, K.V., 2000. Influence of anionic layer structure of Fe-oxyhydroxides on the structure of Cd surface complexes. J. Colloid Interface Sci. 228, 306–316. http://dx.doi.org/10.1006/JCIS.2000.6922.
Maniquiz-Redillas, M.C., Kim, L.-H., 2016. Evaluation of the capability of low-impact development practices for the removal of heavy metal from urban stormwater runoff. Environ. Technol. 37, 2265–2272.
McKenzie, E.R., Money, J.E., Green, P.G., Young, T.M., 2009. Metals associated with stormwater-relevant brake and tire samples. Sci. Total Environ. 407, 5855–5860. http://dx.doi.org/10.1016/j.scitotenv.2009.07.018.
Müller, A., Österlund, H., Marsalek, J., Viklander, M., 2020. The pollution conveyed by urban runoff: A review of sources. Sci. Total Environ. 709, 136125. http://dx.doi.org/10.1016/j.scitotenv.2019.136125.
Na Nagara, V., Sarkar, D., Barrett, K., Datta, R., 2021. Greening the gray infrastructure: Green adsorbent media for catch basin inserts to remove stormwater pollutants. Environ. Technol. Innov. 21, 101334. http://dx.doi.org/10.1016/j.eti.2020.101334.
Nagar, R., Sarkar, D., Makris, K.C., Datta, R., 2010. Effect of solution chemistry on arsenic sorption by Fe- and Al-based drinking-water treatment residuals. Chemosphere 78, 1028–1035. http://dx.doi.org/10.1016/j.chemosphere.2009.11.034.
Papageorgiou, S.K., Kouvelos, E.P., Favvas, E.P., Sapalidis, A.A., Romanos, G.E., Katsaros, F.K., 2010. Metal–carboxylate interactions in metal–alginate complexes studied with FTIR spectroscopy. Carbohydr. Res. 345, 469–473. http://dx.doi.org/10.1016/J.CARRES.2009.12.010.
Punamiya, P., Sarkar, D., Rakshit, S., Datta, R., 2013. Effectiveness of aluminum-based drinking water treatment residuals as a novel sorbent to remove tetracyclines from aqueous medium. J. Environ. Qual. 42, 1449–1459.
Rafatullah, M., Sulaiman, O., Hashim, R., Ahmad, A., 2010. Adsorption of methylene blue on low-cost adsorbents: A review. J. Hazard. Mater. 177, 70–80. http://dx.doi.org/10.1016/J.JHAZMAT.2009.12.047.
Rahman, Z., Singh, V.P., 2019. The relative impact of toxic heavy metals (THMs) (arsenic (As), cadmium (Cd), chromium (Cr)(VI), mercury (Hg), and lead (Pb)) on the total environment: an overview. Environ. Monit. Assess. 191, 1–21. http://dx.doi.org/10.1007/s10661-019-7528-7.
Rajapaksha, A.U., Vithanage, M., Weerasooriya, R., Dissanayake, C.B., 2012. Surface complexation of nickel on iron and aluminum oxides: A comparative study with single and dual site clays. Colloids Surf. A 405, 79–87. http://dx.doi.org/10.1016/J.COLSURFA.2012.05.001.
Reddy, K.R., Xie, T., Dastgheibi, S., 2014. Adsorption of mixtures of nutrients and heavy metals in simulated urban stormwater by different filter materials. J. Environ. Sci. Health A 49, 524–539.
Reed, B.E., Nonavinakere, S.K., 1992. Metal adsorption by activated carbon: Effect of complexing ligands, competing adsorbates, ionic strength, and background electrolyte. Sep. Sci. Technol. 27, 1985–2000. http://dx.doi.org/10.1080/01496399208019460.
Reich, T.J., Koretsky, C.M., 2011. Adsorption of Cr(VI) on γ-alumina in the presence and absence of CO2: Comparison of three surface complexation models. Geochim. Cosmochim. Acta 75, 7006–7017. http://dx.doi.org/10.1016/j.gca.2011.09.017.
Sarkar, D., Na Nagara, V., Datta, R., 2020. Method for generating a granular, green sorbent media for filtration of contaminated water by processing aluminum-based drinking water treatment residuals.
Sharma, S., 2015. Heavy metals in water. R. Soc. Chem. http://dx.doi.org/10.1039/9781782620174.
Shimabuku, K.K., Kearns, J.P., Martinez, J.E., Mahoney, R.B., Moreno-Vasquez, L., Summers, R.S., 2016. Biochar sorbents for sulfamethoxazole removal from surface water, stormwater, and wastewater effluent. Water Res. 96, 236–245. http://dx.doi.org/10.1016/J.WATRES.2016.03.049.
Sidhu, V., Barrett, K., Park, D.Y., Deng, Y., Datta, R., Sarkar, D., 2020. Wood mulch coated with iron-based water treatment residuals for the abatement of metals and phosphorus in simulated stormwater runoff. Environ. Technol. Innov. 21, 101214. http://dx.doi.org/10.1016/j.eti.2020.101214.
Smičiklas, I., Onjia, A., Raičević, S., Janaćković, D., 2009. Authors' response to comments on factors influencing the removal of divalent cations by hydroxyapatite. J. Hazard. Mater. 168, 560–562. http://dx.doi.org/10.1016/j.jhazmat.2009.01.137.
Søberg, L.C., Winston, R., Viklander, M., Blecken, G.T., 2019. Dissolved metal adsorption capacities and fractionation in filter materials for use in stormwater bioretention facilities. Water Res. X 4. http://dx.doi.org/10.1016/j.wroa.2019.100032.
Soleimanifar, H., Deng, Y., Barrett, K., Feng, H., Li, X., Sarkar, D., 2019. Water treatment residual-coated wood mulch for addressing urban stormwater pollution. Water Environ. Res. 91, 523–535. http://dx.doi.org/10.1002/wer.1055.
Soleimanifar, H., Deng, Y., Wu, L., Sarkar, D., 2016. Water treatment residual (WTR)-coated wood mulch for alleviation of toxic metals and phosphorus from polluted urban stormwater runoff. Chemosphere 154, 289–292. http://dx.doi.org/10.1016/j.chemosphere.2016.03.101.
Stumm, W., 1992. Chemistry of the Solid-Water Interface: Processes At the Mineral-Water and Particle-Water Interface in Natural Systems. John Wiley & Son Inc.
Tran, H.N., You, S.J., Hosseini-Bandegharaei, A., Chao, H.P., 2017. Mistakes and inconsistencies regarding adsorption of contaminants from aqueous solutions: A critical review. Water Res. 120, 88–116. http://dx.doi.org/10.1016/j.watres.2017.04.014.
Turner, T., Wheeler, R., Stone, A., Oliver, I., 2019. Potential alternative reuse pathways for water treatment residuals: Remaining barriers and questions—a Review. Water Air Soil Pollut. 230, 1–30. http://dx.doi.org/10.1007/S11270-019-4272-0/TABLES/9.
Wang, X.S., Huang, J., Hu, H.Q., Wang, J., Qin, Y., 2007. Determination of kinetic and equilibrium parameters of the batch adsorption of Ni(II) from aqueous solutions by Na-mordenite. J. Hazard. Mater. 142, 468–476. http://dx.doi.org/10.1016/J.JHAZMAT.2006.08.047.
Weber, Jr., W.J., Morris, J.C., 1963. Kinetics of adsorption on carbon from solution. J. Sanit. Eng. Div. 89, 31–59.

Wen, X., Du, Q., Tang, H., 1998. Surface complexation model for the heavy metal adsorption on natural sediment. Environ. Sci. Technol. 32, 870–875. http://dx.doi.org/10.1021/ES970098Q.

Xie, X., Giammar, D.E., Wang, Z., 2016. MINFIT: A Spreadsheet-based tool for parameter estimation in an equilibrium speciation software program. Environ. Sci. Technol. 50, 11112–11120. http://dx.doi.org/10.1021/ACS.EST.6B03399.

Xu, D., Lee, L.Y., Lim, Y., Lyu, Z., Zhu, H., Ong, S.L., Hu, J., 2020. Water treatment residual: A critical review of its applications on pollutant removal from stormwater runoff and future perspectives. J. Environ. Manage. 259, 109649. http://dx.doi.org/10.1016/j.jenvman.2019.109649.

Zhao, Y., Liu, R., Awe, O.W., Yang, Y., Shen, C., 2018. Acceptability of land application of alum-based water treatment residuals – An explicit and comprehensive review. Chem. Eng. J. 353, 717–726. http://dx.doi.org/10.1016/J.CEJ.2018.07.143.

Zhao, X., Zhang, G., Jia, Q., Zhao, C., Zhou, W., Li, W., 2011. Adsorption of Cu(II), Pb(II), Co(II), Ni(II), and Cd(II) from aqueous solution by poly(aryl ether ketone) containing pendant carboxyl groups (PEK-L): Equilibrium, kinetics, and thermodynamics. Chem. Eng. J. 171, 152–158. http://dx.doi.org/10.1016/j.cej.2011.03.080.